

An Algorithm for Designing of Cascaded Helical Flux Compression Generator

Mohammad Jafarifar^a, Behrooz Rezaeealam^{a,*}, and Ali Mir^a

^a Department of Electrical Engineering, Lorestan University, Khorramabad, Iran

*e-mail: rezaee.bh@lu.ac.ir

Received June 17, 2019; revised June 17, 2019; accepted August 10, 2019

Abstract—Cascaded helical flux compression generators (Cascaded-HFCG) are widely used to produce powerful current pulses in many industries, while there is no specific method to design these generators in any books or articles. In this paper, firstly some mechanical and electrical criteria are described, and then an algorithm is proposed based on these criteria. A computer code is written using MATLAB based on the proposed algorithm and some programs are prepared in COMSOL to calculate electrical parameters of the generators which can be used in the design procedure. The validity of the proposed algorithm is verified by simulation.

DOI: 10.1134/S0020441220010066

1. INTRODUCTION

With the progress of using the HFCGs and Cascaded-HFCGs in many industries and applications, in recent decades, providing a systematic approach to design these generators is essential. Although, in a few papers, some aspects of designing of these generators are described, but most of them are very general about HFCG and didn't mention the details. Almost we can say that there is no reference to design the Cascaded-HFCG in the open literature [1–3].

Since HFCG has a single-shut operation and explosive nature, to reduce the manufacturing costs and achieving the desired current gain and output pulse characteristic it should be designed very accurate and optimized. To optimize the design of any physical system, it is necessary to model that system behavior accurately. Although, there are many approaches to model HFCGs, most of them cannot model some aspects of the HFCG simultaneously like as: armature and winding contact pint loss, flux penetration on the armature wall loss, armature turn skipping from the windings and so on. For these reasons, we have to use some moderate factors in these models, which cause a decrease in accuracy [4–6].

In Cascaded-HFCG, the design process becomes more complicated because of the addition of a second winding that has an important role in the energy transfer between two stages of the generator. Some criteria in Cascaded-HFCG are similar to HFCG such as radius of the generator, mechanical parameters, high explosive selection, and so on. But in some others such as the length of the windings and number of winding sections, the problem will be completely different. Unfortunately, in articles and books, the criteria for

designing Cascaded-HFCG generators have not been mentioned in details. For this reason, most of the generators are not desirable in terms of efficiency and output pulse characteristics. In this paper, the main purpose is to provide an algorithm to simply design the Cascaded-HFCGs and to optimize some parts of these types of generators.

The design process of Cascaded-HFG includes three steps: the selection of suitable explosive to achieve desired explosion velocity, mechanical aspects such as armature design and electrical design like as windings parameters (number of turns, length, the radius of the winding, diameter of the used wire in windings and so on). High explosive selection is an important challenge in the design procedure, because choosing the best one can minimize the size of the generator and explosion pressures and provide the desirable output characteristic too [7]. Table 1 demonstrates some characteristics of the useful high explosive. It should be noted that although these characteristics are considered as constant for each explosive, many factors can change them. Some factors which affecting the characteristics of explosives are: a little change in the chemical composition, temperature of starting explosion, the size of the crystals, the initial density of the solid explosive, and so on.

Between the features mentioned in Table 1, the explosion velocity and the produced mechanical pressures are very important in the design procedure; because the rise-time of output current is proportional to explosion velocity from one hand, and the generator stability during operation is related to the mechanical pressures from the explosion on 8 km/s. Therefore, the

Table 1. Physical characteristics of some explosives [7]

High explosive	Power density, GW/m ²	Energy density, GJ/m ³	Explosion pressure, GPa	Explosion velocity, km/s	Density, g/cm ³
PBX 9501	9.7×10^{-4}	11.0	37	8.8	1.84
Composition B	6.8×10^{-4}	8.6	29.5	8.0	1.72
TNT	5.5×10^{-4}	7.8	21.5	7.0	1.6
EL 5060	4.9×10^{-4}	7.0	20.5	7.0	1.48
Baratol	4.0×10^{-4}	7.8	14.0	5.1	2.6
Nitromethane	4.0×10^{-4}	6.4	12.5	6.2	1.13

first one of the criteria for the maximum explosion velocity is close to 8 km/s or a number lower than that.

2. DESIGN CRITERIA FOR ARMATURE

It can be said that the armature is the most important mechanical component in HFCG. The armature can do more than one task simultaneously in HFCG, which express the importance of the precise and optimal design of this part of the generator. The main tasks of the armature in an HFCG are:

(a) The inner space of an armature acts as an environment to exchange chemical energy of the high explosive to kinetic energy.

(b) The armature acts as an electrical conductor between the windings and the load of the generator to close the electrical circuit. For this purpose, the armature should be made of the high conductivity materials such as copper and aluminum [8].

(c) The expanding armature moves along the windings and wipes out winding turns, which cause to compress the magnetic flux and produce a current pulse.

(d) The armature is used to trap the primary magnetic flux produced by the power supply that is compressed during the generator operation. Although some part of the flux penetrates in the armature wall during compression, it is considered as constant for theoretical analysis.

In an HFCG, the efficiency of the chemical energy conversion to the electromagnetic energy is very low and is approximately close to 10% [9]. There are five reasons that cause to a great amount of energy losses. One of the main goal of the design of the armature is to minimize these losses. The first part of the magnetic flux loss is due to the penetration of flux on the armature wall, which is inevitable in HFCG. A portion of the magnetic flux in the space between the armature and the winding penetrates into the surface layer of the armature during the compression process and lost. This surface layer is called the skin layer. Usually, the term "skin depth" is used to express this type of the flux loss. It should be noted that in the design of

HFCG, the thickness of the armature wall should be considered more than the skin depth. A well-known relationship is presented by Gover and his friends to determine the skin depth of the armature [10]:

$$\delta(t) = \sqrt{\frac{S}{2\mu\sigma u}} \left(1 - \Gamma \frac{t}{t_0}\right), \quad t_0 = \frac{S}{u}, \quad (1)$$

where $\delta(t)$ is skin layer depth; t_0 is starting time of the compression; S is the distance between the inner surface of winding and the outer surface of armature; u is radial velocity of the armature expansion; σ and μ are conductivity and permeability of the armature material; Γ is derivative of skin depth reduction. Using Eq. (1) for calculation the depth of the skin layer is very complicated and, therefore should be replaced by more practical relationships. In the following, a more practical relationship will be presented to calculate the depth of the skin layer.

The second part of the armature losses is due to the inhomogeneity or asymmetry of the armature expansion, which can be eliminate or minimized by optimal design of the armature. It is clear that if the armature jumps over some winding turns (i.e., without connecting one or more turns moves to the turn after them) consequently, the magnetic flux is lost. This phenomenon is called turn-skipping. The turn-skipping occurs when the armature and the winding are not completely coaxial or the armature expansion is carried out heterogeneously, which can be due to improper positioning of the detonator, or the asymmetric distribution of explosives in the internal volume of the armature. In the manufacturing process, an allowed range should be considered for the non-axially between armature and windings to prevent the occurrence of the turn-skipping. This allowed range is called Eccentricity Tolerances. At first it was proposed to determine the maximum tolerance as one of the design criteria as [8]:

$$\Delta a \leq \frac{P}{2} \tan \theta, \quad (2)$$

where Δa is non-axially between armature and windings; P is winding pitch and θ is armature expansion angle.

In 1986, Chernychev and his colleagues presented a newer criterion with more stringency. According to that, the allowed range of non-axially is considered to be much smaller [8]:

$$\Delta a \leq \frac{P}{2\pi} \tan \theta. \quad (3)$$

The third part of the armature losses can be due to the phenomena such as cracks in the armature surface or the very low wall thickness of the armature. For example, the presence of a small gap at the armature surface will weaken the connection between armature and winding turns at that point and cause the flux to be lost. It can also be shown that with the expansion of the armature, the thickness of the wall decreases, which, if not taking into account the depth of the skin layer, will cause flux penetration into the interior of the armature and increase the losses [11–13].

The fourth part of HFCG losses is due to a phenomenon which called the end effect of the armature. In HFCG, generally, an explosion starts from one side using a detonator. At starting of the explosion, a time is required for the formation of the pressure caused by the explosion and conical expansion of the armature. Since the end of the detonator is in free space, a part of the pressure resulting from the explosion is transferred to the free space. This causes to the first section of the armature does not expand completely. Therefore it expands as a bell-shaped rather than conical shape. Due to the non-simultaneously connection between different parts of bell-shape to helical winding, a portion of the magnetic flux is trapped outside the working volume and lost. For this reason, the designers should pay special attention to the effects of the end of the armature and consider several initial turns of winding out away from the range of the end effect. The length L_D , mm, of the end effect of the armature is considered as the distance between the starting points of the explosion to the top of the bell-shaped part in the direction of the armature axis, and can be calculated from the following equation [8]:

$$L_D = c_1 w + c_2 r_A, \quad (4)$$

where r_A is the armature radius, w is the armature wall thickness; c_1 and c_2 are two constants. For copper armature, these constants are 6.8 and 0.219, and 1.72 and 0.266 for aluminum [8].

The fifth part of the flux loss is due to the occurrence of a complex phenomenon at the point of contact between the armature and the winding. In HFCG, the armature contacts to the winding and moves along that. At the point of contact, the copper core of the winding and its insulation, are exposed to an electrical tension, which results in the loss of a portion of the flux. This type of flux losses is inevitable in HFCG, and there is almost no exact relationship to calculation of that [14, 15].

3. DESIGN CRITERIA FOR HELICAL WINDINGS

In the design procedure of helical winding of an HFCG, three rules have to be considered [16]:

(a) Constant voltage rule (constant intensity of the electric field): According to this rule, the internal voltage must not exceed a maximum value (which is considered one of the main design criteria). The investigations show that by increasing the internal voltage to a value higher than 125 kV, the electrical stress on the different parts of the generator increases, especially in electrical insulations therefore, it can lead to electrical failure, which makes to unpleasant performance [17]. However, by adding high-pressure insulating gases such as SF₆, the chance of electric failure reduces but, a maximum of 100 kV is considered for maximum internal voltage in HFCG, which can be increased to 150 kV for Cascaded-HFCG [17–20].

(b) Constant linear current density rule (constant intensity of the magnetic field): Usually, to avoid increasing flux losses due to the nonlinear behavior of the armature and the wires in HFCG, the linear current density is limited to 0.2 MA/cm [21].

(c) Containment rule: The radial displacement of the wires in each section of the winding during flux compression must be less than the maximum Eccentricity Tolerances described in the previous section [21].

3.1. Parameter Selection of First Stage Winding

Given that the current of an HFCG has a pulse form and near-exponential behavior, so as far as the end of the generator operation is approaching, the amplitude of the current increases rapidly. For this reason, if the cross-section of the wire at the end is same as at the beginning, the winding may melt before the end of the generating operation. To overcome this problem, the cross-sectional area of the used wire should be small at the beginning, and becomes larger when it goes toward the end of the generator. The practical implementation of this idea is not so easy and requires sophisticated grinding. An alternative approach for solving the mentioned problem is using a multi-section winding. In this method, the winding is divided into several sections, and in each section, the cross-section is considered suitable amount for the amplitude of current. Nowadays, in new designs for HFCG, instead of changing the cross-sectional area of the wire in different sections, parallel current paths are used. Actually, instead of increasing the cross-sectional area of the wire, several parallel wires (parallel paths) with a smaller cross-section are used.

In an HFCG, in addition to the cross-section, the number of turns and the pitch of winding in each section is also important and affects the output efficiency and output characteristic. To clarify this, we first define the figure of merit coefficient as follows [8]:

$$\beta = 1 + \frac{R}{dL/dt}, \tag{5}$$

where R represents the total ohmic and non-ohmic loss, dL/dt is the rate of inductance change of the winding, which has a negative sign (with the operation of the armature, the turns of the winding wipes out of the circuit and the inductance decreases). Clearly, the larger dL/dt results in the more figure of merit. To increase the value of dL/dt , the pitch of winding should be as large as possible, which reduces the turns of the winding in each section and decreases the initial inductance of the generator. Since the current and energy efficiency of HF CG is directly related to the initial inductance of winding [1], therefore the smaller initial inductance results smaller efficiency. For this reason, in a multi-sectional winding, the pitch of winding in the initial sections is reduced as much as possible, and the pitch is increased towards the end of the generator. It should be noted that the smaller pitch of winding increases the turn-skipping phenomenon and therefore, the minimum pitch of winding has a limitation.

A study of Cascaded-HF CG shows that usually, the first stage winding consists of 3 or 4 sections that in each section the pitch of winding is approximately twice as much as the previous one [22–24]. It should be noted that the last section of the first stage winding is the primary of the transformer, which acts as the load of the first stage. Of course, there is another criterion for calculating the number of sections that are mostly used for HF CG, not for Cascaded-HF CG. Considering the fact that the current at the end of each section is twice as much as the previous one, we can consider the following relation for the current of the sections:

$$\begin{aligned} \frac{I_2}{I_1} = \dots = \frac{I_{i+1}}{I_i} = \dots = \frac{I_n}{I_{n+1}} = 2; \\ \rightarrow \frac{I_n}{I_1} = 2^n \rightarrow n = \log_2^{(I_n/I_1)}, \end{aligned} \tag{6}$$

where I_n is the current of n -th section and I_1 is the current of the first section or input current from the seeding system.

From Eq. (6), we can obtain the number of sections of helical winding to twice increase in current of two adjacent sections. Also, to simplify and achieve a smoother characteristic of the inductance change, the length of all sections are usually considered the same, although this assumption does not affect the overall problem. If the pitch of winding in each section is twice of the adjacent section and assuming the same length for all sections, the number of turns of each section can be obtained from the following equation:

$$\left. \begin{aligned} P_1 = \frac{l_1}{N_1}, \dots, P_n = \frac{l_n}{N_n} \\ l_1 = \dots = l_n \\ P_{i+1} = 2P_i \end{aligned} \right\} \rightarrow N_1 \tag{7}$$

$$= 2N_2 = 4N_3 = \dots = 2^{n-1}N_n,$$

where P_i , l_i and N_i , respectively, represents the pitch of winding, the length and number of turns of the i -th section and n is the number of sections. Usually, the number of turns in the last section of the first stage winding is considered a number between four and eight [22–24]. The further number of turns for the primary winding of the dynamic transformer, due to the high number of parallel paths of current in this section, can lead to bulking of the winding and increase the diameter of the generator, which is not very desirable. Given that the current increment in two adjacent sections is twofold, so the number of parallel paths for passing the current in the two adjacent sections must have a doubly increment. Usually, for the first section of the winding, one current path is considered, and for the n -th section, the number of parallel paths is equal 2^{n-1} .

An important issue related to HF CG is the determination of the diameter or cross-sectional area of the used wire. In a helical, an insulator is used around the wire in order to prevent the electrical breakdown between adjacent turns. Since the internal voltage of the HF CG can sometimes increase to 150 kV, so the used insulation should have high electrical strength but low thickness. Experimental results indicate that in HF CG and Cascaded-HF CG which manufactured so far, the solid insulators like as Teflon or Mylar are well equipped to withstand the produced electric fields [17, 25]. Also, the maximum thickness required to prevent electrical breakdown between the adjacent turns is considered to be 0.5 mm, which is considered as a criterion for insulating thickness in the design of HF CG [17, 25]. Considering a maximum insulation thickness of 0.5 mm, we can easily calculate the diameter of the wire used for winding according to the following equation:

$$D_{wire1} = \frac{l_1}{N_1} - 2 \times 0.5, \tag{8}$$

where D_{wire1} is the diameter of the wire; l_1 and N_1 are the length and the number of turns of winding. The term after the negative sign is due to the thickness of the insulation. If the insulating thickness is taken into account another number, it will be replaced.

3.2. Parameter Selection of Second Stage Winding

By referring to various articles, one can find that for the second stage of a Cascaded-HF CG, a minimum operating time is considered. This minimum time is close to 10 μ s for many applications [23]. On the other

hand, as previously discussed, the explosion velocity is dependent on the type and characteristics of the explosive and is 8200 m/s as maximum. Considering these constraints for the second stage operation time and the explosion velocity, the length of the second stage can be calculated from the following equation:

$$l_{second} = v_{explosion} t_{final}. \quad (9)$$

Since, for the purpose of reducing the rise time of the output pulse, the length of the second stage is much shorter than the first stage, the second stage winding has usually one section. To provide a smoother inductance profile, the diameter of winding (diameter of the generator) should not exceed 1.5 times the length of each section [21]. So:

$$D_{winding} \leq 1.5l_{second}, \quad (10)$$

where $D_{winding}$ is the generator diameter and l_{second} is the length of the second stage that can be calculated from Eq. (9). The diameter of the winding has a minimum possible value. The minimum possible diameter of the winding is determined by the maximum linear current density of the generator [21]. Therefore, the minimum diameter of the winding can be obtained from the following equation:

$$\min(D_{winding}) = \frac{I_m}{2\pi J_{max}}, \quad (11)$$

where I_m is the maximum current and J_{max} is maximum linear current density that is considered 0.2 MA/cm for HFCCG.

Since the energy transfer between the two stages of a Cascaded-HFCCG is carried out by the dynamic transformer, the mutual inductance between the primary and the secondary must be optimal. Experimental results from manufactured generators show that in order to achieve optimal energy transfer between two stages, the following condition must be established between turns of primary and secondary stages of the dynamic transformer [22–24]:

$$N_s > 4N_p, \quad (12)$$

where N_s and N_p are the turn number of the second stage and the first stage winding of dynamic transformer. Using N_s and l_s , the pitch of the second stage winding can be calculated as follow:

$$P = \frac{l_{second}}{N_s}. \quad (13)$$

The diameter of the wire used for the second stage winding considering the thickness of the insulator can be calculated from the following equation, same as the first stage one:

$$D_{wire} = \frac{l_{second}}{N_s} - 2 \times 0.5. \quad (14)$$

3.3. Calculation of the Minimum Cross-sectional Area for the Second Stage According to the Thermal Point of View

Investigating the performance of Cascaded-HFCCG shows that in the final section of the generator, the amplitude of the current increases strongly, therefore inappropriate cross-section may cause to melting the winding before the end of the generator operation, and the output will be undesirable. To achieve a criterion for determining the minimum cross-sectional area of the wire, we first approximate the output current exponentially [26]. That's mean:

$$i_2(t) = I_0 e^{\frac{t}{\tau}}, \quad (15)$$

where τ is the time constant that will be expressed in the follows. Considering t_F as the end time of the generator operation, the final current is equal to:

$$i_2(t_F) = I_F = I_0 e^{\frac{t_F}{\tau}}. \quad (16)$$

Experimental studies show that the thermal losses generated by the current in a copper conductor lead to a limitation in the integral of current action. The integral J of current action is defined as follow:

$$J = \int_0^{t_F} \frac{i_2^2(t)}{S_e} dt = \frac{1}{S_e} \int_0^{t_F} i_2^2(t) dt, \quad (17)$$

where S_e is effective cross-section of current.

The value of the integral of current action is the determinant for the metal phase and for the solid phase is equal to (up to the instant of melting) [27]

$$J_{max} = 0.80492 \times 10^{17} \text{ A}^2 \text{ s/cm}^4. \quad (18)$$

With the value of J_{max} and t_F being known and the current profile, the minimum value for the effective surface of the wire can be calculated. It should be noted that the cross-section calculated from Eq. (14) should not be less than the value obtained in Eq. (17). Otherwise, the cross-section of the wire is considered equal to the value obtained in relation Eq. (17).

3.4. Determination of the Armature Radius, the Depth of the Skin Layer, the Thickness of the Armature Wall

The current passing through the expanding armature can lead to cracking on its surface, which will result in loss of energy and inadequate generator operation. Experimental results and X-ray photography show that the expansion of the armature to 2.13 times the initial radius does not lead to cracking in armature surface [8]. Therefore, if the initial radius of the armature is considered to the half of the radius of the winding, with the expansion of the armature and the increase of its radius to twice the initial value, the best

contact between the armature surface and the winding turns is made. The expansion ratio of the armature is considered as the ratio of the radius of the winding to the initial radius of the armature:

$$a = \frac{r_c}{r_a}, \quad (19)$$

where a is usually equal to 2. Therefore, the optimal radius of an armature is equal to half of the radius of winding which can be calculated from Eq. (10) and Eq. (11).

As mentioned in the previous section, the thickness of the armature wall should be greater than the depth of the skin layer, due to the loss occurred by the penetration of the magnetic flux into the armature wall. Using Eq. (1) to calculate the depth of the skin layer is not very possible because the derivative of the skin layer reduction is not distinguished, therefore more practical relationships should be used to calculate of that. Since the depth of the skin layer is dependent on the frequency, therefore the frequency of the generator must be calculated to determine the depth of the skin layer and also to calculate the electrical resistance of the generator windings. The concept of the frequency as defined for alternating waveforms and since the waveform of output of the helical generator has a pulse form, therefore it is not possible to determine the frequency for that. For this purpose, an average frequency can be used which, in order to calculate that, it is necessary to obtain harmonic components of the output waveform with the help of the Fourier series expansion, and calculate the average frequency from them. On the other hand, the waveform of the HFCG output cannot be expressed analytically. In some cases, with the approximation of the output waveform as an exponential function, the average frequency of the generator can be calculated. In some another case, instead of using the average frequency, the concept of equivalent frequency is used, which is, in fact, the physical interpretation of the average frequency, and can be calculated from the following equation [8]:

$$f = \frac{dI(t)/dt}{\pi I(t)}. \quad (20)$$

It is obvious that using the above equation also needs to know the output waveform of the generator. In the design procedure of an HFCG, usually the equivalent frequency is considered to be the worst case, which is equal to 100 kHz [22]. Considering the equivalent frequency of the generator, the depth of the skin layer, and also the characteristic time constant of the HFCG can be obtained using the following relations [28]:

$$\delta = \frac{1}{\sqrt{\pi f \sigma \mu_0}}; \quad (21)$$

$$\tau = \delta^2 \sigma \pi \mu_0, \quad (22)$$

where δ , τ , σ and μ_0 are respectively, the depth of the skin layer, the time constant of the generator, the conductivity of the armature and the magnetic permeability of the vacuum.

With a simple analysis, it can be shown that the minimum of the armature wall in order to prevent a cracking in the armature surface after expansion can be calculated from the following equation [29]:

$$w_i = r_a \left(1 - \sqrt{1 + \frac{w_f^2 - 2r_c w_f}{r_a}} \right), \quad (23)$$

where r_a and r_c are initial and final armature radius; w_i and w_f are initial and final armature wall thickness. It should be noted that the minimum value of w_f is equal to the skin depth which can be calculated from Eq. (21).

Another important limitation for an HFCG is the maximum current of the armature. By determining the armature radius and the maximum linear current density of the armature, the maximum current of the armature can be calculated as follows:

$$I_{\max} = (2\pi r_a) J_{\max}. \quad (24)$$

In the design process of an HFCG, the current of armature should not be greater than the value obtained from the above equation.

3.5. Maximum Internal Voltage and dI/dt

The internal voltage is one of the design criteria for an HFCG, which is produced by the inductance and current changes. The operation of an HFCG can be expressed using the below equation:

$$\frac{dL}{dt} I + L \frac{dI}{dt} + RI = 0, \quad (25)$$

where R is the total loss of the generator and L is the instantaneous inductance of the helical winding.

The expression $(dL/dt)I$ denotes the internal voltage due to the inductance changes. As mentioned before, the maximum internal voltage to prevent electric breakdown between the generator parts is 150 kV which can be considered less than that depending on the type and size of the generator.

The expression $(dI/dt)L$ is also another part of the produced voltage. It is obvious that the amplitude of this voltage is proportional to the variations of the current in the generator. To prevent the electrical breakdown in generator, dI/dt has a maximum value. In many references, the maximum value of dI/dt is considered in the range [24]

$$10^{11} \leq \frac{dI}{dt} \leq 3.5 \times 10^{11} \text{ A/s}. \quad (26)$$

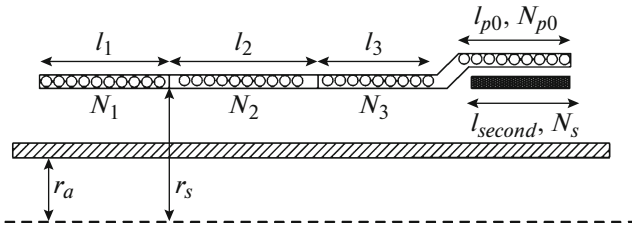


Fig. 1. A schematic of Cascaded-HFCG.

4. DESIGN PROCEDURE OF CASCADED-HFCG

In the previous sections, the main required criteria for the design of different parts of a Cascaded-HFCG were presented. Some of these criteria are empirically obtained using the experiments; therefore the results may not be optimal. As mentioned, there are many criteria for designing a Cascaded-HFCG, so choosing the appropriate values between these criteria, as well as choosing an appropriate algorithm for design, would be a very complicated task. In this section, an algorithm is proposed for the proper selection of the Cascaded-HFCG's parameters to achieve the desired output characteristic. In order to implement the proposed algorithm, a computer program is written using MATLAB. During the execution of this program and in order to calculate the first and second current of the generator, the electrical model presented in [22] is used. In this model, some coefficients are used to account for non-ohmic losses, while there is no theoretical relationship to calculating them. The amount of these coefficients in the proposed algorithm is selected based on references [22, 30, 31]. Also, the self-inductance, mutual inductance, and resistances profiles of the windings, are required to calculate the current in each instant of generator operation. For this reason, a three-dimensional finite element model is prepared in COMSOL software that is called during the execution of the algorithm program for calculation the inductance and resistance profile.

At the beginning of the design process, at first, a schematic of the generator is considered which shown in Fig. 1. As mentioned in Section 3.1, it should be better to build up a Cascaded-HFCG with a maximum of four sections in the first stage and a further increase in the sections number is not recommended due to the complexity of the assembly process.

Figure 2 illustrates the cut-off schematic of the generator in the COMSOL. The COMSOL model is executed in every iteration of the algorithm and calculates the inductance and resistance profiles of the winding taking into account the dynamics of the armature, as well as the effects such as magnetic penetration and so on.

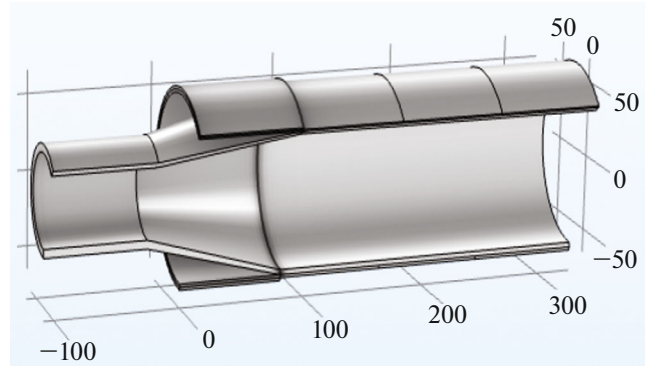


Fig. 2. 3D Schematic of Cascaded-HFCG in COMSOL.

At the beginning, some parameters must be given as input to the algorithm such as the output current I_f , inductance and resistance of the load L_{load}, R_{load} , detonation velocity $v_{detonation}$ and the capacity of seeding capacitance.

As we know, in many applications of HFCG and Cascaded-HFCG, a time range is considered for the output pulse. In many references, the minimum time for the output pulse is considered $t_f = 10 \mu s$ [23]. Thus the second stage length l_s is calculated having $v_{detonation}$ and t_f as

$$l_s = v_{detonation} t_f \tag{27}$$

Using Eqs. (10), (11) and calculated l_s , a permissible range for the winding diameter (diameter of the generator) can be obtained. On the other hand, it can be shown that the larger length-to-diameter ratio of a winding, results the greater inductance [32]. Therefore, the design algorithm considers the amount of winding diameter as the worst possible (maximum value) and reduces the amount of that during the algorithm iterations. Having the amount of winding diameter and using the Eq. (19), the diameter of the armature is also obtained. On the other hand, using the characteristics of explosives from Table 1 and Graney's equation [8], the armature expansion angle can be calculated.

After calculating the length of the second stage winding, the next step is calculating the number of turns of this winding. Since there is no equation for calculation of N_s , the proposed algorithm changes the amount of N_s based on the Eq. (12) and during the design process, until to achieve the desired output characteristic. In order to use the Eq. (12), it is necessary to determine N_{p0} . For this purpose, with the help of a loop in the program, N_{p0} gets the minimum value and then N_s is determined. If during the design process, the output current, the maximum internal voltage, etc., are out of allowed range, the value of N_{p0} will be increased and the program will be restarted.

Table 2. Designing results for 100 kA and 50 kA generators

Design parameter generator	Seeding voltage, kV	Internal voltage 1, kV	Internal voltage 2, kV	r_s , mm	r_a , mm	L_s , mm	L_p , mm
100 kA	1.034	17.6	148.6	147.4	73.8	196.8	590.4
50 kA	3.01	19.02	140.26	111.6	55.8	148.8	446.3
Design parameter generator	D_1 , mm	D_2 , mm	N_s , turns	N_{p0} , turns	N_1 , turns	N_2 , turns	N_3 , turns
100 kA	2.514	3.016	49	7	56	28	14
50 kA	1.324	2.099	48	8	64	32	16

After calculating the parameters of the second stage, the next step is calculating the first stage parameters. In order to straightforwardly and simplicity of the design process, the length of the first stage sections should be considered the same, although this assumption will not affect the subject. It can be said that:

$$L_1 = L_2 = L_3 = L_{p0}. \tag{28}$$

According to Eq. (7), the relation between the turns of first stage sections is as follows:

$$N_1 = 2N_2 = 4N_3 = 8N_{p0}. \tag{29}$$

At the beginning of the first stage operation, since the current is not very high, then one current carrying path is enough. Knowing N_1 and using Eq. (8), the diameter of the used wire for winding can be calculated. It should be noted that in a real generator, the pitch of winding should be taken into account, which makes the Eq. (8) to change a little. In the proposed algorithm, since the some parameters are computed with the help of trial and error, so using approximate relations does not affect the design process. The number of current paths in sections two to four is equal to

2, 3, and 4, respectively [20–24]. From Eq. (29), the number of turns of the first sections is obtained, followed by the diameter of the wire, and so on.

After calculating the turns of the first and second stage winding, their length and other parameters, these values are given to the finite element model and the inductances and resistances profiles are obtained again. At the end, with the help of inductance and resistance profiles and using the Cascaded-HFCG electrical model, the first and second stage current profiles in terms of time are calculated. Given the current profiles and the inductances and resistances of the windings, it is possible to calculate the produced internal voltage and dI/dt . Also, using the current profiles of the first and second stages align with Eq. (17) and Eq. (18), it is possible to obtain the cross-sectional area (or diameter) of the wire used for the winding in terms of thermal constraints. The obtained value is compared with the value obtained from Eq. (14) and finally, the biggest one is considered as the cross-sectional area of wire.

Within the main body of the program, there are several other loops that, during the design process, examine each of the constraints raised for the generator. These constraints are the maximum output current, the maximum internal voltage, the minimum pitch, the depth of skin layer, and the minimum thickness of armature wall, etc. The flowchart of the proposed algorithm is presented in appendix. Due to the long and bulky algorithm, the flowchart is presented in several separate sections.

5. SIMULATION RESULTS AND DISCUSSION

As we have seen, in this paper an algorithm was proposed for the design of Cascaded-HFCG. Since in almost no book or article, one can find a specific pattern for designing this kind of generator, the proposed algorithm can be very useful in designing and reducing the manufacturing costs of cascaded-HFCG. In order to evaluate the performance of the proposed algorithm, the design of a cascaded-HFCG to produce a

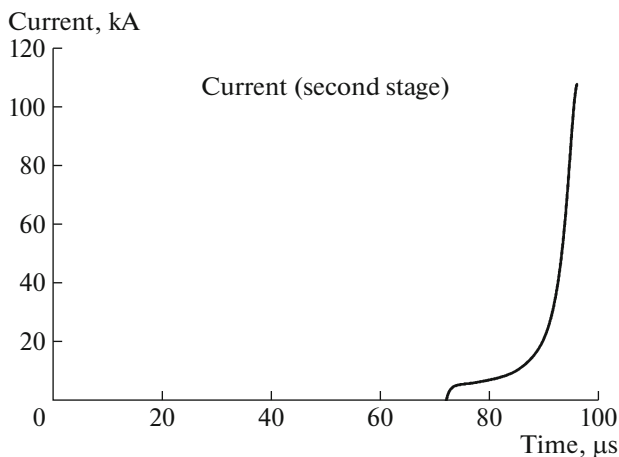


Fig. 3. Load current-100 kA generator.

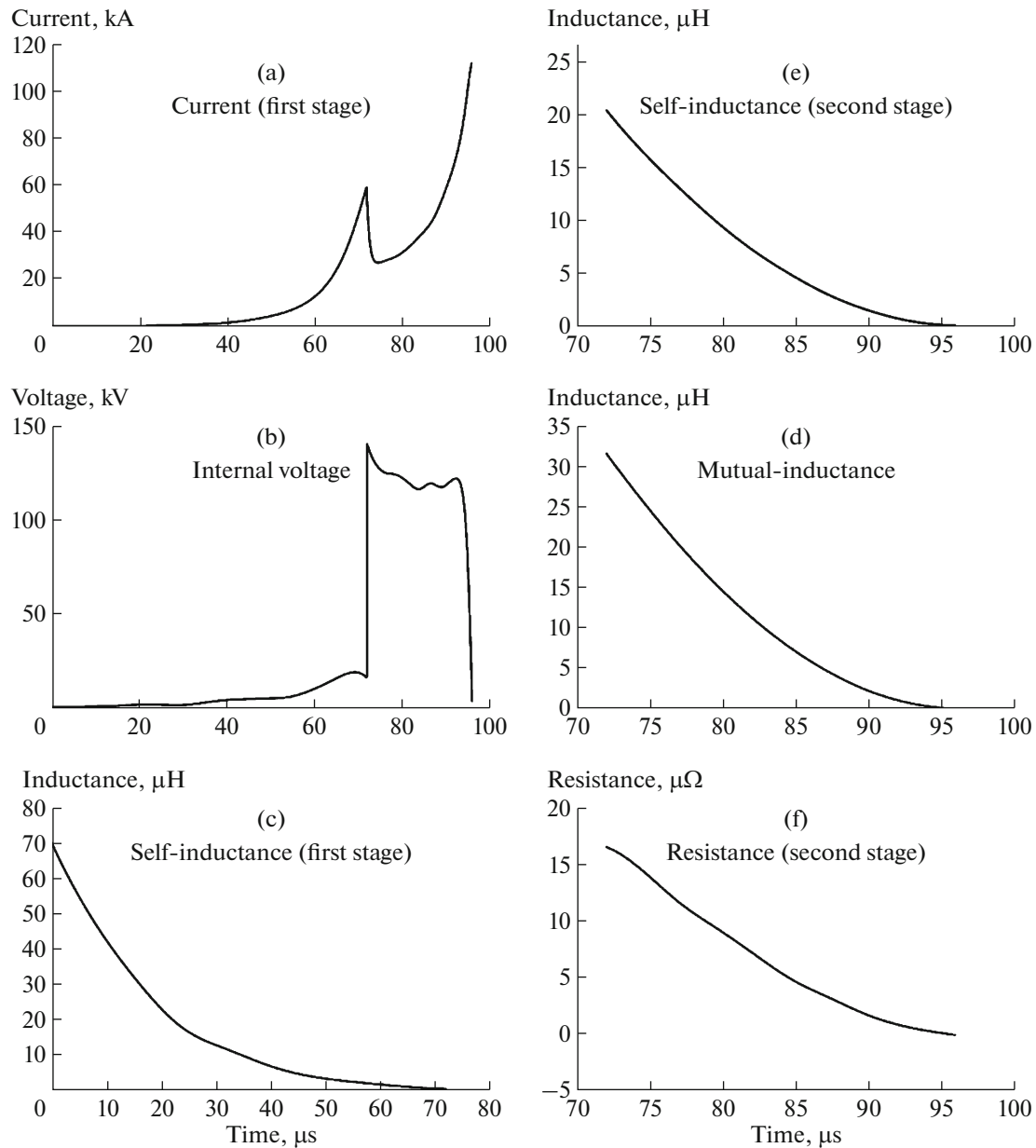


Fig. 4. Simulation results-100 kA Generator.

current pulse with 100 kA amplitude is considered in this section. The load current of 100 kA, 100 μH load inductance, 0.01 Ω load resistance and detonation velocity of 8200 m/s are given as the input information. The operation time of the second stage, which is the rise time of the output pulse, is also in the range of 10 to 24 μs . This time starts from the minimum value at the beginning of the algorithm and, if necessary, will increase. Table 2 shows the outputs of the design algorithm for the considered generator. It should be noted that the mentioned results are obtained after 37 iterations of the algorithm to achieve the desired output.

Investigating the results of Table 2, shows that the obtained N_s and N_{p0} satisfy the Eq. (12), which means the maximum energy transfer occurs between two stage windings by the dynamic transformer. Figure 3 demonstrates the output current profile obtained from the computer simulation. As we can see, the load current amplitude is close to 100 kA. The operation time of the second stage is calculated from the crowbar instant to the complete destruction of a generator that is close to 20 μs , which is acceptable for many applications of Cascaded-HFCG.

One of the most important design parameters in an HFCG is the thickness of the armature wall. If its

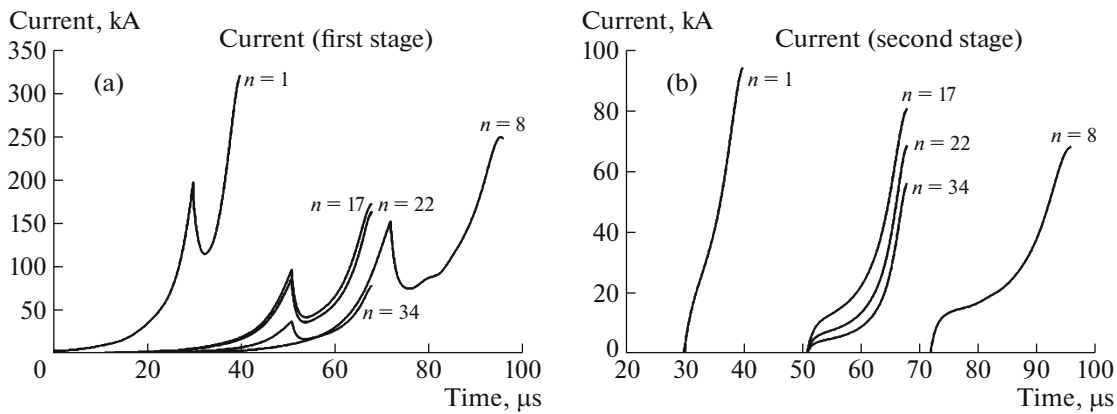


Fig. 5. First and second stage currents-50 kA generator. n is the number of iteration of simulation program.

amount is not suitable, the magnetic flux penetrates the surface of the armature and affects the generator operation performance. The algorithm calculates the thickness of the armature wall about 13.9 mm. On the other hand, the depth of the skin layer for the worst working frequency (100 kHz) and for the armature made of aluminum and copper is given by Eq. (21), respectively: 0.2593 and 0.2061 mm. Therefore, the thickness of the armature wall obtained by the algorithm is acceptable.

Figure 4a-f shows the other generator variables including the first stage current, the internal voltage, the self-inductance of the first and second stages and their mutual inductance, as well as the resistance of the second stage winding. It is clear from the internal voltage diagram that its maximum is close to 148 kV, which is lower than its maximum limit. These results indicate that the design is acceptable in terms of internal voltage.

In the follow of this section, the designing of a cascaded-HFCG with the current pulse of 50 kA amplitude is carried out. The practical information of the proposed generator is given in [22]. This generator delivers a current pulse with 50 kA amplitude to a load of 2.68 μ H inductance and 30 m Ω resistance. Table 2 shows the parameters obtained for the different sections of this generator. The further number of the turns in the first stage winding leads to an increase in the initial inductance of the first stage and a decrease in the rate of the inductance changes, consequently, leads to a lower final current of the first stage than the manufactured generator in [22].

Figure 5a,b shows the current of the first and second stage of the generator. As it can be seen, the current of the first stage is limited to a value less than 100 kA while, this current is raised to about 300 kA in Ref. [22]. Since the current of the first stage does not get to the load, cause to increase the ohmic loss of generator and decrease in efficiency. The rise-time of current obtained by the algorithm is about 15 μ s, while its

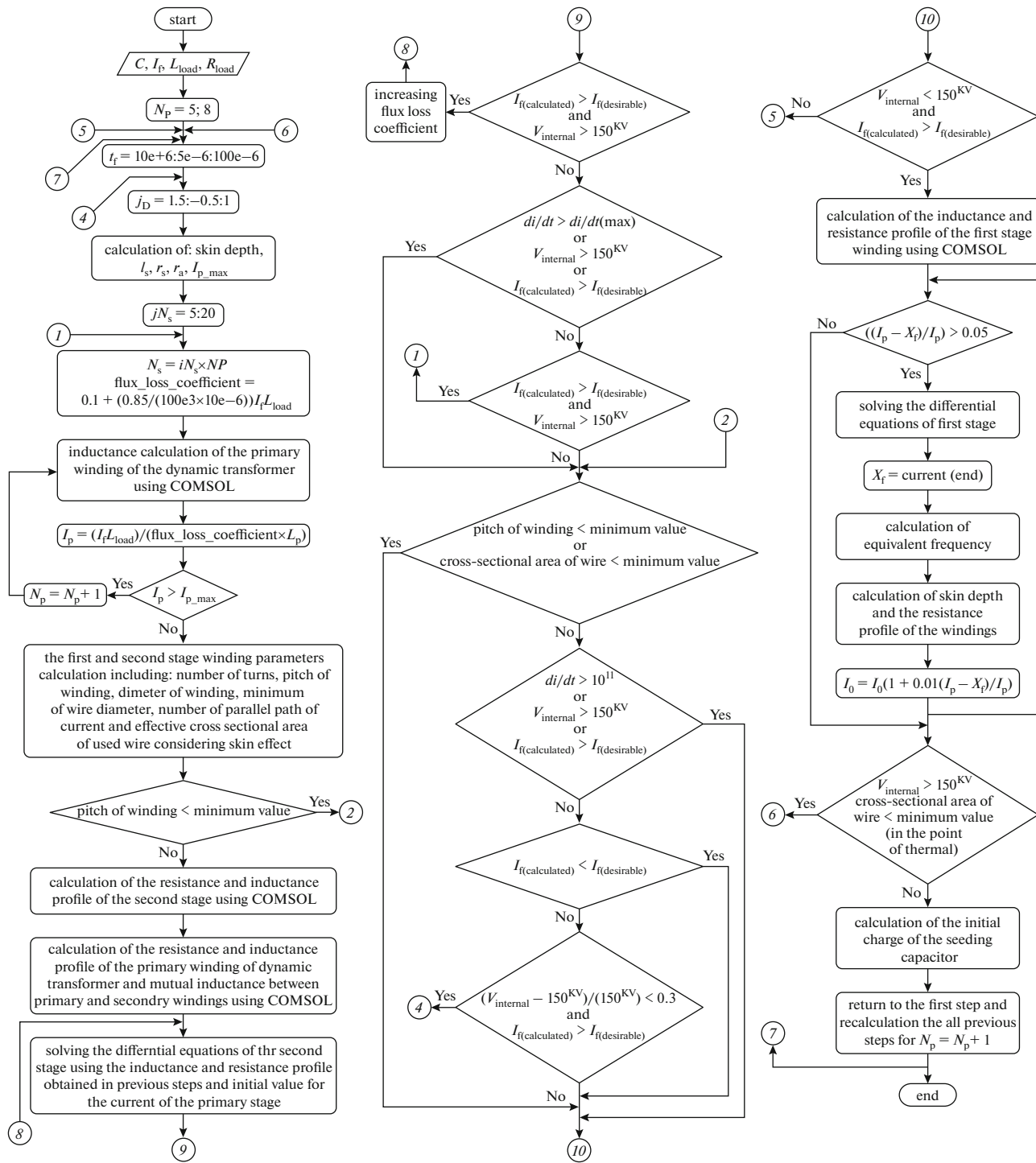
practical value is close to 10 μ s. The main reason for this difference is that the practical generator in [22] has a conical form end, which will increase the amount of dI/dt , consequently, decrease the rise-time of current. Generally, the cone-shaped end of the generator in cascaded-HFCG is one of the approaches to reduce the rise-time of current, which has been addressed in various references [30].

6. CONCLUSION

With the increasing advances in the use of HFCG in different sciences and industries in recent years, it is necessary to provide an algorithm for designing these generators. There are many design criteria for these types of generators but, there is no specific pattern for appropriate selection of these criteria in papers and books. In this paper, the essential criteria for designing and manufacturing of Cascaded-HFCG are presented. In order to optimize the design process, a design algorithm is proposed. The simulation results are presented in several sections and it can be seen that the proposed algorithm largely satisfy the requirements in relation with the design process of HFCG. The simulation results show that in the first stage of the generator, the maximum value of the current is lower than the conventional one, which helps to decrease the ohmic loss and consequently to increase the generator efficiency. Most of the limitation related to the practical implementation of the generators include the internal voltage, the minimum pitch of winding, the minimum thickness of the armature wall, and so on are also considered in this algorithm.

APPENDIX

The flowchart of the proposed algorithm in this paper is as follows:



REFERENCES

1. Altgilbers, L.L., Grishnaev, I., Smith, I.R., Tkach, Y., Brown, M.D.J., Novac, B.M., and Tkach, I., *Magneto-cumulative Generators*, in *Magneto-cumulative Generators*, New York: Springer, 2000. https://doi.org/10.1007/978-1-4612-1232-4_3.
2. Atchison, W.L., Goforth, J.H., Lindemuth, I.R., and Reinovsky, R.E., *Proc. 12th IEEE Int. Pulsed Power Conference*, Monterey, CA, 1999, p. 332. <https://doi.org/10.1109/PPC.1999.825478>
3. *Magneto-cumulative Generators—Pulsed Energy Sources*, Demidov, V.A., Plyashkevich, L.N., and Selemir, V.D., Eds., Sarov: Russian Federal Nuclear Center – All-

- Russian Scientific Research Institute of Experimental Physics, 2012, vol. 1, p. 231.
4. Freeman, J.R., McLaughlin, J.M., Thompson, S.L., and Cnare, E.C., in *Megagauss Physics and Technology*, Boston, MA: Springer, 1980, p. 205.
 5. White, D.A., Rieben, R.N., and Wallin, B.K., *Proc. Int. Conference on Megagauss Magnetic Field Generation and Related Topics, Herlany*, November 5–10, 2006, p. 371.
<https://doi.org/10.1109/MEGAGUSS.2006.4530704>
 6. Kiuttu, G.F., Chase, J.B., Chato, D.M., and Peterson, G.G., *Proc. Int. Conference on Megagauss Magnetic Field Generation and Related Topics, Herlany*, November 5–10, 2006, p. 255,
<https://doi.org/10.1109/MEGAGUSS.2006.4530686>
 7. Agrawal, J.P., *High Energy Materials: Propellants, Explosives and Pyrotechnics*, Weinheim: John Wiley and Sons, 2010.
 8. *Explosively Driven Pulsed Power, Helical Magnetic Flux Compression Generators*, Neuber, A.A., Ed., Berlin, Heidelberg: Springer, 2005.
 9. Herlach, F., *Pulsed Magnetic Field Generators and Their Practical Application*, in *Megagauss Physics and Technology*, New York: Springer, 1980, p. 1.
<https://doi.org/10.1007/978-1-4684-1048-8>
 10. Gover, J.E., Stuetzer, O.M. and Johnson, J.L., *Megagauss Physics and Technology*, Boston, MA: Springer, 1980, p. 163,
https://doi.org/10.1007/978-1-4684-1048-8_15.
 11. Baird, J. and Worsey, P.N., *Proc. 28th IEEE Int. Conference on Plasma Science and 13th IEEE Int. Pulsed Power Conference*, Las Vegas, NV, June 17–22, 2001, vol. 1, p. 94.
<https://doi.org/10.1109/PPPS.2001.960709>
 12. Baird, J., Worsey, P.N., and Schmidt, M., *Proc. 28th IEEE Int. Conference on Plasma Science and 13th IEEE Int. Pulsed Power Conference*, Las Vegas, NV, June 17–22, 2001, vol. 1, p. 953.
<https://doi.org/10.1109/PPPS.2001.960830>
 13. Baird, J. and Worsey, P.N., *IEEE Trans. Plasma Sci.*, 2002, vol. 30, no. 5, p. 1647,
<https://doi.org/10.1109/TPS.2002.805379>
 14. Kiuttu, G.F. and Chase, J.B., *Proc. IEEE Pulsed Power Conference*, Monterey, CA, 2005, p. 435.
<https://doi.org/10.1109/ppc.2005.300682>
 15. Haurylavets, V.V. and Tikhomirov, V.V., *Math. Models Comput. Simul.*, 2013, vol. 5, no. 4, p. 334.
<https://doi.org/10.1134/S2070048213040054>
 16. Novac, B.M. and Smith, I.R., *Electromagn. Phenom.*, 2003, vol. 3, no. 4, p. 490.
 17. Demidov, V.A., *IEEE Trans. Plasma Sci.*, 2010, vol. 38, no. 8, p. 1773.
<https://doi.org/10.1109/TPS.2010.2049751>
 18. Pavlovskii, A.I., Lyudaev, R.Z., Zolotov, V.A., Seryoghin, A.S., Yuryzhev, A.S., Kharlamov, M.M., Shuvalov, A.M., Gurin, V.Ye., Spirov, G.M., and Makaev, B.S., in *Megagauss Physics and Technology*, Boston: Springer, 1980, p. 557.
https://doi.org/10.1007/978-1-4684-1048-8_53.
 19. Chernyshev, V.K., Zharinov, E.J., Demidov, V.A., and Kazakov, S.A., in *Megagauss Physics and Technology*, Boston: Springer, 1980, p. 641.
https://doi.org/10.1007/978-1-4684-1048-8_58.
 20. Novac, B.M., Enache, M.C., Smith, I.R., and Stewardson, H.R., *Laser Part. Beams*, 1997, vol. 15, no. 3, p. 397.
<https://doi.org/10.1017/S026303460001096X>
 21. Novac, B.M., Smith, I.R., Stewardson, H.R., Senior, P., Vadher, V.V., and Enache, M.C., *J. Phys. D: Appl. Phys.*, 1995, vol. 28, no. 4, p. 807.
<https://doi.org/10.1088/0022-3727/28/4/027>
 22. Wang, Y., Zhang, J., Chen, D., Cao, S., Li, D., and Liu, C., *Rev. Sci. Instrum.*, 2013, vol. 84, no. 1, p. 014703.
<https://doi.org/10.1063/1.4775488>
 23. Dong-Qun Chen, *PhD Dissertation*, Changsha Univ., 2015.
 24. Shurupov, A.V., Fortov, V.E., Koslov, A.V., Leont'ev, A.A., Shurupova, N.P., Zavalova, V.E., Dudin, S.V., Mintsev, V.B., and Ushnurtsev, A.E., *Proc. 14th Int. Conference on Megagauss Magnetic Field Generation and Related Topics (MEGAGAUSS-2012)*, Maui, Hawaii, October 14–19, 2012, p. 1.
<https://doi.org/10.1109/MEGAGAUSS.2012.6781431>
 25. Anderson, C.S., Neuber, A.A., Young, A.J., Krile, J.T., Elsayed, M.A., and Kristiansen, M., *Proc. IEEE Pulsed Power Conference*, Chicago, IL, 2011, p. 513.
<https://doi.org/10.1109/PPC.2011.6191476>
 26. Appelgren, P., *Licentiate Dissertation*, Stockholm: KTH Royal Institute of Technology, 2008.
 27. Tucker, T.J. and Toth, R.P., EBW1: A Computer Code for the Prediction of the Behavior of Electrical Circuits Containing Exploding Wire Element, Albuquerque, NM: Sandia National Laboratories, 1975.
<https://doi.org/10.2172/4229184>
 28. Appelgren, P., *Doctoral Thesis*, Stockholm: KTH Royal Institute of Technology, 2011.
 29. Bola, M.S., Madan, A.K., and Singh, M., *Def. Sci. J.*, 1992, vol. 42, no. 3, p. 157.
<https://doi.org/10.14429/dsj.42.4375>
 30. Freeman, B.L., Boydston, J.C., Ferguson, J.M., Lindenburg, B.A., Luginbill, A.D., and Tutt, T.E., *Proc. 14th IEEE Int. Pulsed Power Conference*, Dallas, TX, 2003, vol. 2, p. 1081.
<https://doi.org/10.1109/PPC.2003.1277999>
 31. Young, A., Neuber, A., and Kristiansen, M., *IEEE Trans. Plasma Sci.*, 2010, vol. 38, no. 8, p. 1794.
<https://doi.org/10.1109/TPS.2010.2048723>
 32. Snow, Ch., *Formulas for Computing Capacitance and Inductance*, Washington, DC: US Government Printing Office, 1954, vol. 544.